Purification and Spectroscopic Characterization of Ctb, a Group III Truncated Hemoglobin Implicated in Oxygen Metabolism in the Food-Borne Pathogen *Campylobacter jejuni*†

Laura M. Wainwright,‡ Yinghua Wang,§ Simon F. Park,|| Syun-Ru Yeh,§ and Robert K. Poole*,‡

Department of Molecular Biology and Biotechnology, The University of Sheffield, Sheffield S10 2TN, U.K., Department of Physiology and Biophysics, Albert Einstein College of Medicine, Bronx, New York 10461, and School of Biomedical and Molecular Sciences, University of Surrey, Guildford GU2 7XH, U.K.

Received November 3, 2005; Revised Manuscript Received March 15, 2006

ABSTRACT: *Campylobacter jejuni* is a food-borne bacterial pathogen that possesses two distinct hemoglobins, encoded by the *ctb* and *cgb* genes. The former codes for a truncated hemoglobin (Ctb) in group III, an assemblage of uncharacterized globins in diverse clinically and technologically significant bacteria. Here, we show that Ctb purifies as a monomeric, predominantly oxygenated species. Optical spectra of ferric, ferrous, O_2- and CO-bound forms resemble those of other hemoglobins. However, resonance Raman analysis shows Ctb to have an atypical ν_{Fe-CO} stretching mode at 514 cm^{-1}, compared to those of the other truncated hemoglobins that have been characterized so far. This implies unique roles in ligand stabilization for TyrB10, HisE7, and TrpG8, residues highly conserved within group III truncated hemoglobins. Because *C. jejuni* is a microaerophile, and a *ctb* mutant exhibits O_2-dependent growth defects, one of the hypothesized roles of Ctb is in the detoxification, sequestration, or transfer of O_2. The midpoint potential (E_h) of Ctb was found to be −33 mV, but no evidence was obtained in vitro to support the hypothesis that Ctb is reducible by NADH or NADPH. This truncated hemoglobin may function in the facilitation of O_2 transfer to one of the terminal oxidases of *C. jejuni* or, instead, facilitate O_2 transfer to Cgb for NO detoxification.

In the past three decades, our understanding of hemoglobins has grown to recognize new classes of proteins in addition to the classical vertebrate α- and β-globins, myoglobin, and the symbiotic hemoglobins (Hbs[1]) of leguminous plants. These new globins, some of which may actually be among the oldest or ancestral globins in a phylogenetic context (*1*), include the nonsymbiotic plant Hbs, chimeric flavohemoglobins, and the trHbs. Globins may be classified functionally, into those that detoxify NO and those that are involved in O_2 transfer or detoxification, or structurally into three categories (*2*). The first structural category contains flavoHbs that possess a *C*-terminal ferredoxin-$NADP^+$ reductase-like domain and an *N*-terminal globin domain; bacterial (*3*, *4*) and yeast (*5*) examples function in the enzymic removal of NO to produce nitrate (*6*, *7*). The second category contains single domain Hbs that are very similar to the *N*-terminal domain of the flavoHbs; however, their functions appear more varied than those of the flavoHbs. For example, Vgb, found in the obligate aerobe *Vitreoscilla*, is believed to function in the facilitation of O_2 transfer to cytochrome *bo′* (*8*), whereas the *C. jejuni* Hb, Cgb, confers tolerance to NO (*9*) and is up-regulated by NO and its congeners by an NO-activated transcriptional regulator (*10*).

The trHbs comprise the third category: members possess an altered structure whereby the globin fold is edited from the three-over-three α-helical sandwich (3/3) characteristic of vertebrate globins to a two-over-two arrangement (*11*) and are sometimes called 2/2 Hbs (*1*). This results in a considerably smaller globin, composed typically of 110−130 amino acids. A subdivision of the trHbs, based on the information available from more than 40 actual or putative trHb genes, was proposed by Wittenberg et al. (*12*). Three distinct groups were identified (I, II, and III), with four subgroups occurring within group II. Few amino acids are strictly conserved throughout the trHb sequences, only the proximal HisF8 being invariant (see below). Note that we use here the terms group I, II, and III in this context as defined by Wittenberg et al. (*12*) and not to distinguish between the truncated globins, myoglobin-like proteins, and flavohemoglobins (*13*).

The crystal structures of trHbs from *Chlamydomonas*, *Paramecium* (*11*), *Mycobacterium tuberculosis* (*14*, *15*), and *Synechocystis* (*16*) have been solved. The antiparallel helix pairs are comprised of B/E and G/H. The A helix is almost entirely deleted, and the instability implied by this absence is remedied by the presence of a hydrophobic amino acid cluster in the AB region to allow efficient sealing of the proximal side of the heme pocket (*11*). There are three

† This work was supported by the Biotechnology and Biological Sciences Research Council (BBSRC, U.K.) through Research Grant D18084 and the National Institutes of Health through NIH Grant HL65465.

* To whom correspondence should be addressed. Phone: (+44) 114 222 4447. Fax: (+44) 114 222 2800. E-mail: r.poole@sheffield.ac.uk.

‡ The University of Sheffield.

§ Albert Einstein College of Medicine.

|| University of Surrey.

[1] Abbreviations: Ctb, *Campylobacter* truncated hemoglobin; Hb, hemoglobin; Mb, myoglobin; MOPS, morpholinopropanesulfonic acid; trHb, truncated hemoglobin; Vgb, *Vitreoscilla* hemoglobin.

10.1021/bi052247k CCC: $33.50
Published on Web 04/18/2006

conserved Gly−Gly motifs located in the AB hinge (*11*), the EF hinge, and at the end of the pre-F loop (*17*), respectively, that are believed to stabilize the globin fold. Only group I and II trHbs possess the Gly−Gly motifs; little is known concerning the putative motifs that replace them in terms of stabilization within group III. The F helix is attenuated to a single turn, the rest being replaced by an extended polypeptide segment termed the pre-F loop (*11*). Group II trHbs have a conserved EF loop, whereas this area in group I trHbs is shorter and lacking in sequence conservation (*18*). The C helix is barely present, and the CD-D region is reduced to approximately three residues, arguably the smallest polypeptide span that could join the C and E helices (*12*).

There are only a few strictly conserved residues within the known trHb sequences. The trHbs, without exception, retain the conserved HisF8 residue as the proximal ligand to the heme. However, the conserved residues of the distal pocket are more variable. At the B9−B10 sites, there is a strongly conserved Phe−Tyr couplet, the TyrB10 being involved in heme ligand stabilization (*12*). Position CD1 is conserved as Phe in group I and III trHbs; those residues in group II inhabiting the position can be Phe, Tyr, or His. The E7 position is more variable: in group I trHbs, the position is occupied mostly by GlnE7, in group III trHbs it is invariably HisE7, and in group II, the position is occupied by Ala, Ser, or Thr. Phe almost always occupies the E14 position in all groups; this residue is believed to shield the heme from the solvent in a role comparable to that of PheCD1 in other hemoglobins (*12*).

The gram-negative microaerophilic bacterium *Campylobacter jejuni* is notable but not unique in possessing two different Hbs. In addition to Cgb, a single-domain (3/3) Hb (*9*), it possesses Ctb (*19*), which belongs to trHb group III. This is by far the least well-understood family of Hbs, despite the fact that it embraces globins (*12*) from the pathogens *Bordatella pertussis* and *Mycobacterium avium* and the obligately aerobic metal-leaching acidophilic bacterium *Thiobacillus ferrooxidans*. *C. jejuni* is now recognized as one of the most important causes of bacterial gastroenteritis worldwide (*20*). In humans, campylobacteriosis is mainly a food-borne disease. However, *C. jejuni* is commonly a gut commensal in many food-producing animals and birds, and the contamination of meat during processing is an important method of transfer (*20*). Cgb protects the bacterium from the toxic effects of NO (*9*), but the group III trHb has no clearly defined function. Its expression is, however, elevated in response to nitrosative stress, a response mediated by the NssR sensor/regulator (*10*). The microaerophilic nature of *C. jejuni* implies the presence of mechanisms for high affinity O_2 binding and/or coping with O_2 toxicity, and it is possible that Ctb fulfils one of these functions (*19*). In the present work, we have cloned and overexpressed the *C. jejuni* Ctb (Cj0465c), characterized it through optical and resonance Raman spectroscopy, and determined its midpoint redox potential. This is the first detailed characterization of a group III trHb.

EXPERIMENTAL PROCEDURES

Bacterial Strains and Culture Conditions. Campylobacter jejuni strain NCTC 11168 was obtained from the National Collection of Type Cultures (London). *E. coli* TOP10 (Invitrogen) was used for the overexpression of Ctb; the expressing strain was named RKP4979. *C. jejuni* strains were grown at 42 °C in a Mueller−Hinton medium in a modular atmosphere controlled system (MACS) VA500 workstation (Don Whitley Scientific) with a constant gas supply of 10% oxygen, 10% carbon dioxide, and 80% nitrogen. The plates were incubated for 48 h; the cells from these were inoculated into 50 mL of liquid culture in a 100 mL flask and grown for approximately 18 h. The apparent absorbance (OD_{600}) was adjusted to 0.5 and cultures reinoculated at 1.33% (v/v) into fresh medium in 250 mL baffled flasks and then grown with shaking at 115 rpm. The Mueller−Hinton medium was supplemented with vancomycin (10 μg/mL). *E. coli* strains were grown in Luria−Bertani (LB) medium at 37 °C at 200 rpm and on nutrient agar at the same temperature. The media were supplemented with ampicillin (50 μg/mL).

Cloning and Expression of C. jejuni trHb in E. coli. Genomic DNA was isolated from *C. jejuni* NCTC 11168 using guanidium thiocyanate (*21*). The forward (RP268, 5′ AAAATTAACATTTAACCATGGCTTATA TG AAATTT-GAAAC-3′) and reverse (RP267, 5′-GAAAAGGTAAA-AAAAGC TTTGGCAAAAAAATTG-3′) primers were designed on the basis of the sequence of the *C. jejuni* genome and contained an NcoI and HindIII site, respectively (underlined). PCR products were visualized on a gel. The 0.38 kb fragment was recovered with a Qiaquick gel extraction kit (Qiagen), cloned between the *Nco*I and *Hin*dIII sites of pBAD/His (Invitrogen) and transformed into *E. coli* TOP10 using the method of Inoue et al. (*22*). The construct was checked by sequencing from just upstream of the promoter through to the end of the insert. For the overexpression, starter cultures grown overnight in LB supplemented with ampicillin were inoculated at 1% (v/v) into 500 mL of LB in 2 L baffled flasks supplemented with ampicillin, 200 μM δ-aminolevulinic acid, and 12 μM $FeCl_3$. The cultures were shaken at 200 rpm until an OD_{600} of $\sim$ 0.5 had been reached; they were then induced with 0.02% arabinose and grown for a further 4 h. Concentrations of δ-aminolevulinic acid, $FeCl_3$, and arabinose were selected after preliminary optimization studies.

Purification of C. jejuni trHb. All buffers used in purification were made up using MilliQ water. Commonly, 4 L of culture were grown for a single purification. The cells were harvested by centrifugation at 5000*g* for 10 min at 4 °C and resuspended in 80 mL of 50 mM Tris-HCl (pH 7.0). The cells were broken by ultrasonication and cell debris removed by centrifugation at 21 000*g* for 15 min at 4 °C. The clear supernatant obtained was reddish brown in color and was loaded onto a 30 mL DEAE Sepharose Fast Flow (Pharmacia Biotech) column equilibrated with 50 mM Tris-HCl (pH 7.0) in an Åkta Purifier (GE Healthcare Bio-Sciences, Amersham Biosciences, U.K. Ltd.). The column was washed with 40 mL of the same buffer and the trHb eluted with a NaCl gradient (from 0 to 0.5 M) in 50 mM Tris-HCl buffer (pH 7.0). The fractions to be carried forward for the next step were chosen on the basis of coincidence of the heme (412 nm) and protein (280 nm) peaks in the UV−visible absorption profile. The eluate was concentrated to $\sim$1.4 mL using a Vivaspin 20 concentrator (Vivascience) with a molecular mass cutoff of 5 kDa. This fraction was further purified by gel filtration. A Superdex-200 column (16 $\times$ 60 cm, GE

Healthcare Bio-Sciences, Amersham Biosciences, U.K. Ltd.) was equilibrated with 50 mM Tris-HCl (pH 7.0) containing 0.2 M NaCl. A 1 mL portion of the previous fraction was applied and eluted in the equilibration buffer at a flow rate of 1 mL/min. Pure Ctb was stored at 4 °C.

O_2 Consumption Studies. A digital Clark-type electrode system (Model 10: Rank Brothers) connected to a chart recorder was used to measure O_2 consumption. Experiments were carried out at 37 °C in a 1.5 mL volume. Na dithionite and air-saturated buffer were used to calibrate the electrode, and experiments with 3.3−9.5 μM Ctb (final concentrations) were performed in a 50 mM K phosphate buffer (pH 7.0). Additions of experimental components were made through the lid with a Hamilton syringe. The pure Ctb used was in the oxygenated form.

Visible Absorbance Spectroscopy. Absorption spectra were recorded using a custom-built SDB4 dual wavelength scanning spectrophotometer (University of Pennsylvania School of Medicine Biomedical Instrumentation Group and Current Designs, Philadelphia, PA) as described by Kalnenieks et al. (*23*). Ctb was reduced using a few grains of Na dithionite. CO binding was achieved by bubbling reduced samples for 2 min with the gas. Samples were oxygenated by passage of reduced globin down a Sephadex G-25 column (Amersham Biosciences) in aerated 50 mM Tris-HCl pH 7.0. Ctb was oxidized using K ferricyanide or ammonium persulfate.

Measurement of Redox Potential. This was carried out at room temperature in the previously described dual wavelength spectrophotometer according to the method of Dutton (*24*) in a custom-built cuvette of 10 mm path length. A ThermoRussell CMMPtR4 Ag/AgCl redox electrode was used (4 M KCl electrolyte). It was calibrated against a solution of 0.1 M K ferrocyanide and 0.05 M K ferricyanide. Oxidized Ctb was obtained by dialysis of the pure protein against 4 L of 50 mM glycine HCl buffer (pH 2.5) at 4 °C overnight with stirring. Ferric Ctb was then dialyzed back into 50 mM Tris HCl at pH 7.0 and used at 9 μM (final concentration) in 50 mM MOPS buffer (pH 7.0) for the titration. The following redox mediators were used at the final concentrations given in parentheses: quinhydrone (*50*); *N*,*N*,*N*′,*N*′-tetramethylene-*p*-phenyldiamine (20 μM); 1,2-naphthoquinone-4-sulfonate (40 μM); naphthoquinone (25 μM); trimethylhydroquinone (20 μM); phenazine methosulfate (12.5 μM); phenazine ethosulfate (20 μM); 1-methyl-1,4-naphthoquinone (20 μM); and 1-hydroxy-1,4-naphthoquinone (25 μM). Ctb was progressively reduced by titration with an anoxic Na dithionite solution, and spectra were recorded approximately every 20 mV. The ΔA value (432−452.5 nm) was measured. Reverse titrations were performed with a K ferricyanide solution. The midpoint potential was determined by plotting the redox potential against % oxidized Ctb/% reduced Ctb. The midpoint potential was taken to be the poise at which % oxidized/% reduced equals 1 (*24*).

Resonance Raman Techniques. The concentration of protein samples used for the Raman measurements was typically 30−100 μM in phosphate-buffered saline. Raman measurements with Soret excitation were taken with previously described instrumentation (*13*, *25*, *26*). Briefly, the 413.2 nm line of a krypton ion laser (Spectra Physics, Mountain View, CA) was used as an excitation source. The laser power was maintained in the 0.5−2 mW range to minimize CO dissociation. The Raman scattered light was dispersed through a polychromator (Spex, Metuchen, NJ) equipped with a 1200 grooves/mm grating and detected by a liquid nitrogen-cooled CCD camera (Princeton Instruments, Princeton, NJ). A holographic notch filter (Kaiser, Ann Arbor, MI) was used to remove laser scattering. Typically, several 10 s (or 1 min) spectra were recorded and averaged after the removal of cosmic ray spikes by a standard software routine (CCD spectrometric multichannel analysis, Princeton Instruments, NJ). Frequency shifts in the Raman spectra were calibrated using indene as the reference. The accuracy of the spectra was approximately ± 1 cm^{-1} for absolute shifts and less than ± 0.25 cm^{-1} for relative shifts.

RESULTS

Sequence Analyses. The *C. jejuni* trHb (accession number Cj0465c) is encoded by an approximately 0.38 kb stretch of DNA. The surrounding DNA encodes an ATP-dependent DNA helicase, a zinc protease-like protein, an ABC transporter and a regulator (NssR), believed to be a distant member of the Crp/Fnr family, that up-regulates both Ctb and Cgb in response to nitrosative stress (*10*).

Figure 1 shows a structure-based alignment of Ctb with several other microbial Hbs. The first eight Hbs are categorized as members of the trHb-III group (*12*) by the highly conserved PheB9, TyrB10, PheCD1, HisE7, PheE14, and HisF8 residues. TrpG8 is also highly conserved in members of group III. In group II trHbs, for instance, the trHbO from *Mycobacterium tuberculosis*, this residue is part of a hydrogen bonding network with TyrCD1 that stabilizes heme-bound ligands (*13*, *15*). Such an interaction is not possible in the *C. jejuni* trHb because the CD1 position is filled by an apolar residue (Phe). The E11 residue is conserved in group III trHbs as leucine or isoleucine. In trHbs of group II, for instance, trHbN from *Mycobacterium tuberculosis* and the trHb from *Chlamydomonas eugametos*, this position is occupied by a polar residue, which is involved in the formation of a hydrogen-bonding network with heme-bound ligands (*11*, *13*, *14*).

Optical Spectra. The *ctb* gene was cloned into pBAD and overexpressed in *E. coli*. Ctb was purified using ion exchange and gel filtration chromatography. The globin eluted from the gel filtration column as a monomer. SDS−PAGE analysis gave an estimated molecular mass of 14 kDa. This is consistent with the theoretical value of 14.06 kDa based on the amino acid composition of the protein. The absolute electronic absorbance spectra of Ctb are displayed in Figure 2. The trHb was found as a mixture of the ferric and oxy forms when isolated (native form). It was characterized by a Soret peak at 411 nm, a broad peak at around 512 nm, a charge transfer band at 640 nm, and two peaks at 542 and 578 nm. In a typical Hb, the ferric heme iron in the resting state is axially coordinated by an exogenous water ligand in the distal position. Because water is a weak field ligand, the heme iron typically exhibits a mixture of six-coordinate high-spin and low-spin configurations. At high pH, the heme-bound water is partially deprotonated, and the contribution from the low-spin component increases because hydroxide is a strong field ligand for the heme iron. The 512 and 640 nm absorption bands found in Ctb are characteristic for a water-bound form with six-coordinate high-spin configuration; the 542 and 578 nm bands signal the low-spin

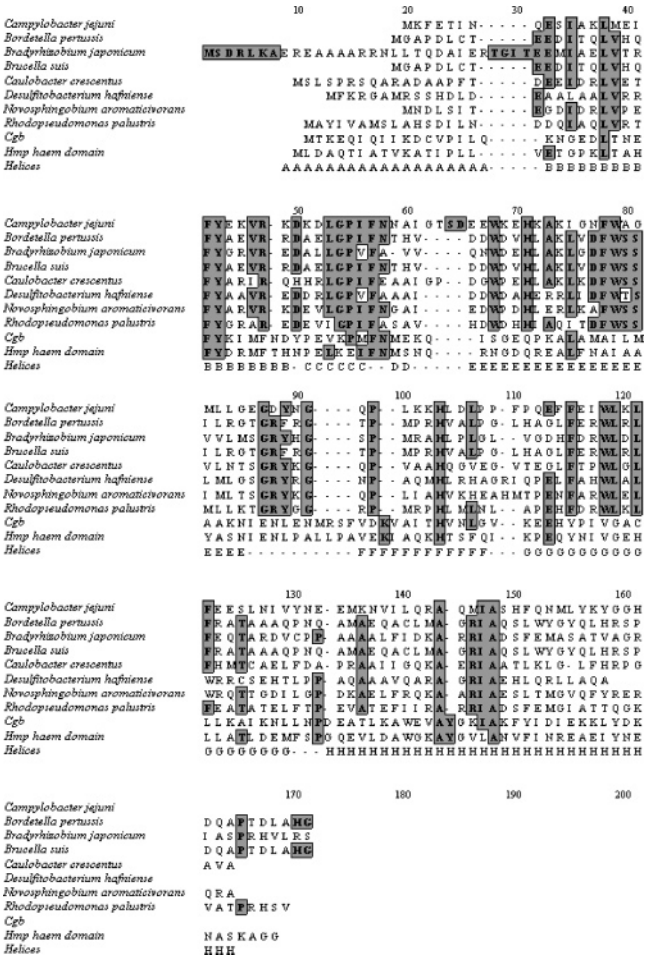

FIGURE 1: Sequence alignment of *C. jejuni* trHb with various trHbs, Cgb, and the Hmp heme domain. The sequence comparison was carried out using Clustal W. The top eight sequences are trHbs, followed by the nontruncated globin (Cgb) of *C. jejuni*, and the *N*-terminal heme domain of *E. coli* flavohemoglobin (Hmp). The locations of the respective helices (A−H) are displayed in the bottom line below the aligned sequences. Conserved residues are shaded. The sequence data for various hemoglobins were obtained from TIGR.

configuration. However, the latter two bands are similar to those of the oxy form (see below). The intensity of these two bands decreased when native Ctb was exposed to an oxidant (K ferricyanide or ammonium persulfate). This oxy component is stable, decaying only gradually over a period of months at 4 °C to a predominantly ferric state.

Pure ferric species was obtained by ferricyanide oxidation under anaerobic conditions and purification using a desalting column. The species exhibits a Soret band at 410 nm and two pairs of bands at 512 and 640 nm and 542 and 582 nm. The ferric species can be slowly reduced by dithionite over a period of ~15 min. The reduced protein displayed a Soret band at 432 nm and a broad $\alpha\beta$-band with a maximum at 565 nm. The addition of carbon monoxide to the reduced form readily resulted in the formation of the carbonmonoxyferroheme. This displayed a narrow Soret band at 421 nm and $\alpha\beta$ bands at 538 and 569 nm, separated by a shallow trough. The oxygenated form was easily made by passage of ferrous Ctb down an aerated PD10 column. The species exhibited a Soret peak at 414 nm and $\alpha\beta$ bands at 542 and 578 nm. A spectrum was scanned of whole *E. coli* cells overexpressing Ctb. The globin was found to be in the oxy

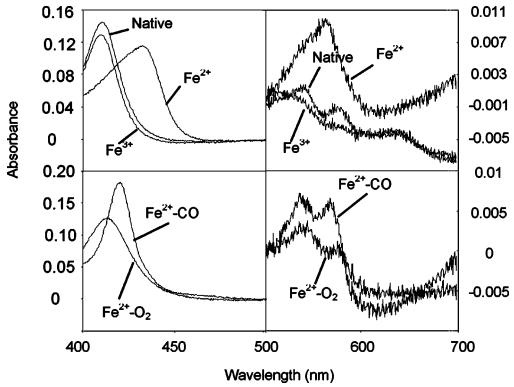

FIGURE 2: Electronic absorbance spectra of pure Ctb. All spectra were scanned against a 50 mM Tris-HCl at pH 7.0 baseline and are normalized to heme concentration (0.001 mM). The native Ctb corresponds to the globin as it elutes from the gel filtration column (peak maxima at 411, 512, 542, 578, and 640 nm). The other forms of Ctb were generated as described in the text. Peak maxima are as follows. Fe^{2+}, 432 and 565 nm; Fe^{3+}, 410, 512, 542, 582, and 640 nm; Fe^{2+}-CO, 421, 538, and 569 nm; and Fe^{2+}-O_2, 414, 542, and 578 nm.

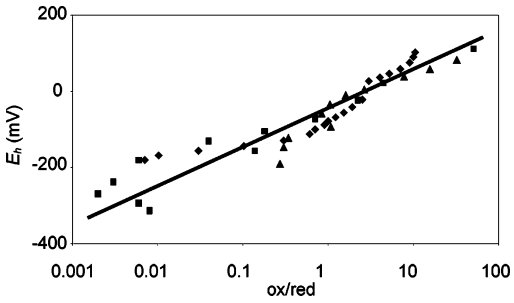

FIGURE 3: Redox titration of Ctb. The electrochemical potential was plotted against % oxidized Ctb/% reduced Ctb in a semilog arithmetic plot according to the Nernst equation. Reducing (♦, ▲) and oxidizing (■) titrations are shown. The line has been fitted to all three titrations ($R^2 = 0.83$).

form (data not shown; see Supporting Information Figure S1).

Redox Titration of Ctb. During the reduction of Ctb, it was observed that the globin was unusually slow in becoming fully reduced, taking approximately 15 min. This can be compared with leghemoglobin and horse heart myoglobin, both of which are fully reduced within a minute of adding dithionite. We postulated that the slow reduction of Ctb might be due to a low midpoint potential.

Controls were performed to ensure the reliability of the titrating system. The midpoint potential of horse heart cytochrome *c* was experimentally determined to be +261 mV. This compares favorably with literature values (+255 mV) (*27*). A blank titration was performed omitting Ctb to ensure that the spectral changes observed during titrations were due to Ctb and not to mediators. The titrations were always performed in the reductive direction because the ferrous form was not reliably generated in significant quantities. The titration was taken from +200 mV to −400 mV to ensure the full reduction of Ctb. Figure 3 displays three titrations performed in both oxidizing and reducing directions. The midpoint potential using the hydrogen electrode as reference is −33 mV.

Resonance Raman Spectra. Figure 4 shows the resonance Raman spectrum of the ferric derivative at pH values 7.0, 9.5, and 10.5. At neutral pH, ferric Ctb shows a typical

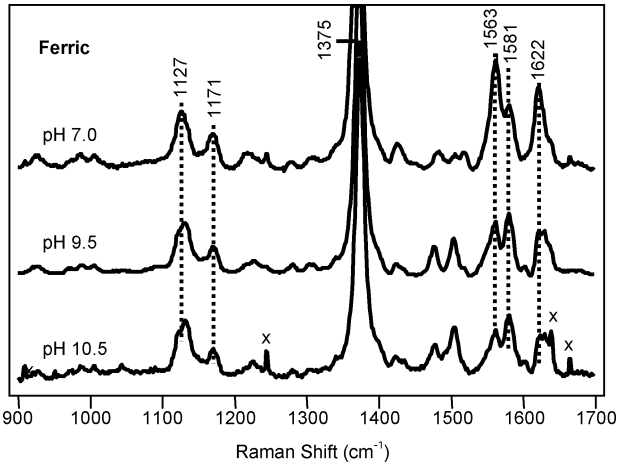

FIGURE 4: Resonance Raman spectra of ferric Ctb. The Raman spectrum of the ferric form was obtained at pH 7.0, 9.5, and 10.5.

mixture of six-coordinate high-spin and low-spin configurations as indicated by the ν_2 modes at 1563 and 1581 cm^{-1}, respectively, confirming that a water ligand is bound to the distal site of the heme. The intensity of the low-spin component, as reflected by the 1581 cm^{-1} band, develops as the pH increases, consistent with the de-protonation of the heme-bound water. The high-spin to low-spin transition is consistent with the optical absorption data, in which the intensities of bands at 542 and 582 nm bands increase with respect to those at 498 and 640 nm as the pH increases (data not shown; see Supporting Information Figure S2).

The ferrous ligand-free form of Ctb exhibits a five-coordinate high-spin configuration as judged by the ν_3 and ν_4 modes at 1471 and 1356 cm^{-1}, respectively. The ν_{Fe-His} mode, which is observable only in the five-coordinated deoxy species, was identified at 226 cm^{-1} (Figure 5, top). It is identical to that of trHbN and trHbO, reflecting a strong iron−histidine bond.

In the high-frequency region of the resonance Raman spectrum of the CO-derivative, ν_4 is located at 1372 cm^{-1}, and ν_3 and ν_2 are located at 1498 and 1583 cm^{-1}, respectively (data not shown; see Supporting Information Figure S3). The spectrum is characteristic of a ferrous six-coordinate heme protein. In the low-frequency region, an isotope sensitive line at 514 cm^{-1} was observed (Figure 5, bottom), which is shifted to 499 cm^{-1} in the $^{13}C^{18}O$ derivative, in accordance with the predicted shift for an Fe−CO diatomic oscillator. In the isotope difference spectrum, all the heme-related modes are canceled out to leave the two ν_{Fe-CO} lines appearing as a positive peak at 517 cm^{-1} for $^{12}C^{16}O$ and a negative peak at 494 cm^{-1} for $^{13}C^{18}O$ (Figure 5, bottom). Likewise, a ν_{C-O} mode was identified at 1936 cm^{-1} on the basis of the isotope substitution experiment (data not shown).

An inverse correlation curve relating the frequencies of the Fe−CO stretching modes with those of the associated C−O stretching modes has been well established owing to the two resonance structures of the Fe−C−O moiety as shown below (*28*−*30*).

$$\text{L-Fe}^{-}\text{-C}{\equiv}\text{O}^{+} \leftrightarrow \text{L-Fe}{=}\text{C}{=}\text{O} \qquad (1)$$

Here, L represents the proximal iron ligand, a histidine in the case of Hbs. In general, a distal environment with positive polar residues destabilizes the form (I), thereby strengthening

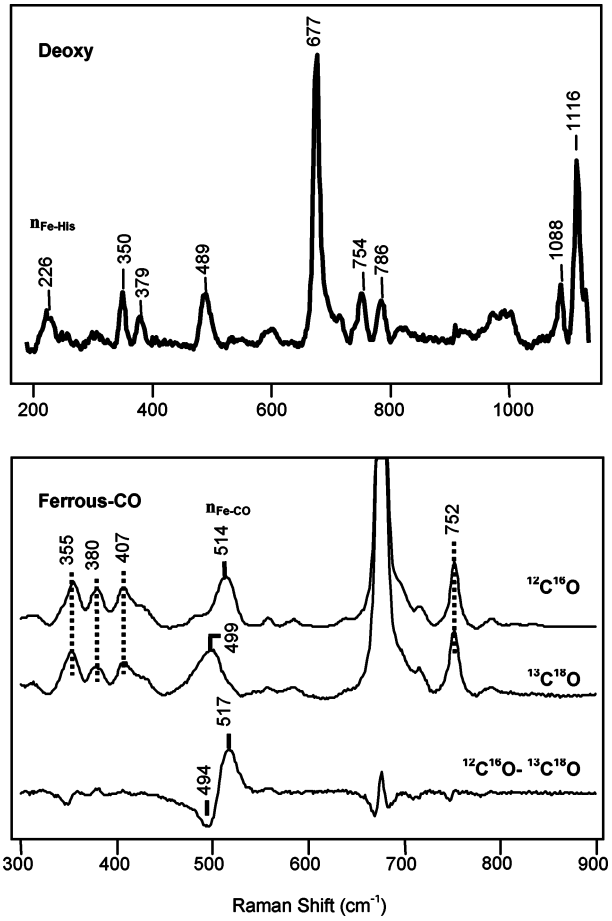

FIGURE 5: Resonance Raman spectra of the ferrous deoxy form (top) and the Fe^{2+}-CO form (bottom) of Ctb.

the Fe−CO bond and concomitantly weakening the C−O bond. However, the identity of the proximal ligand L affects the electronic properties of the Fe−C−O moiety such that the curve for the imidazole/histidine coordinated species is distinct from that of the thiolate coordinated species and that of the five-coordinate CO adduct. The CO-bound form of Ctb falls on the imidazole/histidine correlation curve (Figure 6), confirming the assignment of the proximal ligand as a histidine.

On the imidazole/histidine correlation curve, the data points for the peroxidases typically locate at the higher left corner of the correlation line because of their polar distal environment. However, those of mammalian globins in general locate at the lower right corner of the correlation line because of the much more hydrophobic distal environment. In Hmp (*E. coli* flavohemoglobin), two conformations were observed. One locates in the Mb region, and the other locates in the peroxidase region, indicating that the distal pocket of Hmp is flexible and fluctuates between an open and a closed conformation. In the closed conformation, the heme-bound CO is stabilized by a H-bonding interaction involving the distal B10 Tyr and/or E7 Gln; this interaction is absent in the open conformation (*31*).

In Vitro Examination of Ctb. In preliminary experiments, supernatant fractions of cell extracts (i.e., with membranes centrifuged out) from *E. coli* overexpressing Ctb displayed double the O_2 consumption of control supernatants (Wainwright, L. M. and Poole, R. K. Unpublished data). To test whether oxygen consumption could be demonstrated for the

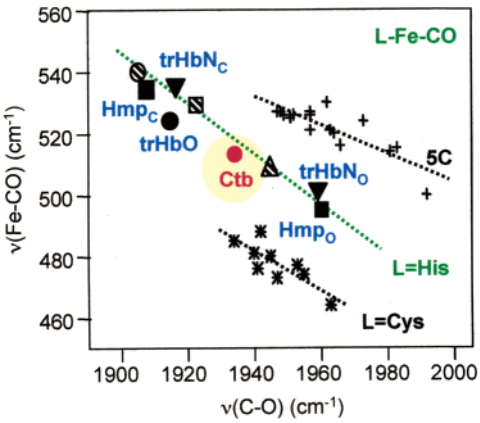

FIGURE 6: Inverse correlation diagram of the Fe−CO stretching frequency versus the C−O stretching frequency of various heme proteins and a comparison with Ctb. The solid inverted triangles represent trHbN in closed (trHbN$_c$, upper) and open (trHbN$_o$, lower) conformations. Nearby, the solid squares represent Hmp in closed and open conformations. TrHbO is represented by the solid, red circle in the top left portion of the plot, and Ctb by the circle in the center of the L = His line. The striped circle (extreme top left), striped square, and striped triangle (middle) represent horseradish peroxidase, cytochrome *c* peroxidase, and Mb, respectively. The L = Cys line corresponds to those proteins where the proximal ligand to the heme is the thiolate side chain of cysteine, the L = His line corresponds to those proteins where the proximal ligand is the imidazole/imidazolate side chain of histidine, and the 5C line corresponds to those proteins where the CO-bound form is pentacoordinate.

purified protein, as with Mb in the presence of methylene blue, NADH, and cytochrome *c* reductase (*32*) or with Hmp (*33*), we used ascorbate (0.5 mM) or NADH (0.5 mM) as electron donors and phenazine methosulfate (PMS, 7 μM) as a redox mediator. However, no O_2 consumption by Ctb alone was observed. Reduction of Ctb was also sought spectrophotometrically. To pure Ctb (100 μg) in 50 mM Tris-HCl at pH 7.0 in an anaerobic glass cuvette were added several redox mediators (PMS, phenazine ethosulfate, and methylene blue, 7 to 21 μM, final concentrations) with reductant (0. 5 mM ascorbate or NADH) and cytochrome *c* reductase (2.7 mg/mL). The spectrum was scanned against a buffer blank for approximately 30 min after the addition of the mediator and reductant. No reduction of Ctb could be demonstrated by these methods, but addition of Na dithionite reduced the protein.

DISCUSSION

Significant advances have been made from crystallographic studies of purified trHbs, complemented by spectroscopic tools, particularly resonance Raman spectroscopy. In combination with site-directed mutagenesis, these methods have yielded important structural insights into some but not all of Wittenberg's groups.

Group I trHbs. The best-studied group I trHb is trHbN, which is expressed in stationary phase cultures of *M. tuberculosis* (*34*). The B10, E7, E10, E11, and E14 positions are occupied by Tyr, Leu, Lys, Gln, and Phe, respectively (reviewed in ref *13*). The importance of TyrB10 in stabilizing heme-bound ligands is well established for several trHbs, including trHbN: mutation to Leu disrupts the H-bonding network and increases the O_2 off-rate by 200-fold (*34*). TrHbN displays ν_{Fe-CO} modes at 534 and 500 cm^{-1} and matching ν_{C-O} modes at 1936 and 1960 cm^{-1}, respectively (*26*), indicating that it has an Hmp-like equilibrium structure with fluctuating open and closed conformations (*13*, *26*, *31*). The ferrous ligand-free derivative of trHbN has a five-coordinate configuration, and the ν_{Fe-His} mode is at 226 cm^{-1} (*26*). Detailed studies on three other group I trHbs, such as trHbC from the green alga *Chlamydomonas eugametos*, trHbS from the cyanobacterium *Synechocystis*, and trHbP from the flagellate protozoan *Paramecium caudatum*, have been recently reviewed elsewhere (*13*).

Group II trHbs. An example of group II is provided by trHbO of *M. tuberculosis*, the second trHb in this bacterium. The most striking feature is the CD1 residue, which is not Phe, as in almost all globins studied to date, but Tyr-36 (*35*). Furthermore, in the dodecameric crystalline state, the B10 Tyr is covalently bonded to the CD1 Tyr in six of the subunits, whereas in the remaining six, the residue side chains are in intimate contact but without the covalent linkage (*15*). This unique CD1/B10 pair creates a rigid distal environment for heme-bound ligands. The ν_{Fe-His} mode is at 226 cm^{-1} (*36*). Unlike trHbN, the CO derivative shows only one ν_{Fe-CO} mode at 525 cm^{-1}, which is assigned to a closed conformation (*35*).

Group III trHbs. Ctb, the subject of this article, is the first group III trHb to be described in detail. The optical spectra of purified Ctb, in general, closely resemble those of hemoglobins. The absorbance of the ferric Soret band is a few nm higher than is typical, but this is not significant. It is interesting that Ctb predominantly purifies in the ferrous-oxy form (Figure 2, S1). Indeed, it would appear that oxygen tightly binds to Ctb because even under anaerobic conditions, the oxy form remains stable for at least a couple of hours. The tight binding of oxygen requires that the protein be deoxygenated prior to oxidation. The Fe−His stretching frequency of Ctb (226 cm^{-1} in Figure 5) is similar to the results obtained for other trHbs, lying between 220 and 232 cm^{-1} (*13*, *25*, *34*, *35*, *37*). In mammalian Hb or Mb, the imidazole ring of the proximal histidine is in an eclipsed orientation with respect to the pyrrole nitrogen atoms of the porphyrin, in contrast to a staggered orientation in the trHbs (*36*). Consequently, the proximal histidine is repelled from the porphyrin ring and results in a weakened proximal iron−histidine bond. This attenuation is manifested by the lower ν_{Fe-His} mode at ~214−220 cm^{-1} (*38*). However, the Fe−His mode of Hmp, the *E. coli* flavoHb, at 244 cm^{-1} is significantly larger than that of Ctb because of a H-bonding interaction between the proximal histidine and a nearby glutamate residue (*13*). The H bond pulls the proton away from the histidine, giving it an imidazolate character. Similar large values of ν_{Fe-His} are found in peroxidases (240−260 cm^{-1}), where the histidine ligand also exhibits imidazolate character (*31*). This H-bonding interaction is not present in any of the trHbs with known structures, consistent with their relatively lower ν_{Fe-His}. Taken together, these observations suggest that the proximal histidine ligand of Ctb has neutral character and has its imidazole ring in a staggered position with respect to the pyrrole nitrogen atoms of the porphyrin ring (*13*, *25*, *31*, *34*−*38*).

Ferrous Ctb under neutral conditions is five-coordinate and high-spin. This trait is displayed in a number of Hbs, including trHbs found in *M. tuberculosis* (*26*, *35*), *Chlamydomonas* (*25*), *Paramecium* (*37*), and the flavoHb Hmp of

E. coli (*31*). Only the trHb found in *Synechocystis* is six-coordinate and low-spin when reduced (*39*).

The Raman characteristics of the CO derivative (Figures 5 and 6) show Ctb to have an atypical ν_{Fe-CO} stretching mode at 514 cm^{-1} compared to those of the other truncated hemoglobins that have been characterized so far (*13*, *26*, *31*). The TyrB10, HisE7, and TrpG8 in Ctb are highly conserved in the group III trHbs, suggesting ligand stabilization roles of these residues in Ctb. The situation in Ctb is different from that in the trHbs of *Chlamydomonas* (*25*), *Paramecium* (*37*) and *Synechocystis* (*39*). In these three globins, the stretching mode of the Fe−CO bond is comparatively low at ∼490 cm^{-1}. This is due to the open nature of the heme pocket, resulting in very little polar interaction of CO with the surrounding residues (*13*, *37*).

Functions of Ctb and Other trHbs. Relatively little functional information is available on the various trHbs so that correlation between the proposed classification and function must remain tenuous. The fact that globins from different groups may coexist in the same organism, as in *C. jejuni* and *M. tuberculosis*, suggests that members of these subgroups are not functionally redundant. Indeed, *Mycobacterium avium* contains three trHbs, one from each subgroup. Lending support to this notion is the fact that the two trHbs of *M. tuberculosis* appear to have distinct functions: trHbN (group I) has been implicated in performing NO/O_2 chemistry and actively detoxifies NO yielding nitrate (*40*−*42*), whereas trHbO (group II) may play a role in oxygen transfer (*18*). Although the very high oxygen affinities of trHbO (*43*) and the *Bacillus subtilis* group II trHb (*44*) appear inconsistent with intracellular oxygen management, recent data reveal the ability of this globin to bind phospholipid membranes with weak affinity for the terminal oxidase, cytochrome *bo′*, of *E. coli* (*45*). Notwithstanding the uncertainty regarding trHbO (group II) function, the *M. leprae* GlbO in group II has been implicated in NO scavenging (*46*).

At present, it seems premature to assign distinct functions to trHb groups I, II, and III. The ancestor of contemporary globins, emerging perhaps 4000 Mya, may have been trHb-like or current single-domain-like (3/3) globins (*1*). It seems likely that such an ancestor evolved to deal with various diatomic ligands (O_2, NO, CO), and that contemporary trHbs preserve this ancient diversity of function, even within the current somewhat arbitrary classification. As for other trHbs, the function of Ctb is ambiguous. On the one hand, a role in oxygen metabolism is indicated by the growth phenotypes of a *ctb* mutant (*19*) and the effects of this deletion on the kinetics of oxidase-catalyzed respiration. The finding that Ctb is oxygenated in whole *E. coli* cells indicates that the high affinity of the oxidases for O_2 (*47*, *48*) presents no obstruction to Ctb binding O_2 in vivo. This parallel with Vgb and also the similarity of the Ctb Raman data to that for trHbO, leads us to hypothesize a role for Ctb in the facilitation of O_2 transfer to the terminal oxidases. The local O_2 concentration of the host environment of *C. jejuni* is most likely to be lower than is ideal for growth of the bacterium. Thus, *C. jejuni* may benefit from possessing an intracellular O_2-concentrating mechanism. However, when *C. jejuni* transfers between hosts, the bacterium will be exposed to significantly higher O_2 levels than those at which it can grow. A mechanism whereby excess O_2 is detoxified might appear beneficial. However, although *C. jejuni* possesses an iron superoxide dismutase encoded by *sodB* (*49*) that would protect against superoxide formation, the stability of the oxyferrous form argues against a reductive detoxification mechanism.

On the other hand, Cgb accumulation is increased on exposure to *S*-nitrosoglutathione (*10*), and transcriptional regulation of the *ctb* gene is mediated in response to nitrosative stress by NssR, a member of the Crp-Fnr superfamily (*10*). However, a *ctb* mutant is not hypersensitive to a range of nitrosative stress-inducing reagents (*19*). If Ctb were to be involved indirectly in NO detoxification, then it may, like Hmp, require reduction for sustained NO reductase or oxygenase (denitrosylase) activity. With a midpoint potential of −33 mV, Ctb appears to be capable of accepting electrons from NAD(P)H (−320 mV), and therefore, an enzymatic activity of Ctb within the cell is not precluded, but we were unable to reduce Ctb in vitro except with dithionite. Ctb may require a specific reductase to feed electrons to the heme iron in vivo. Indeed, Frey et al. (*50*) could not demonstrate NO consumption activity from *E. coli* overexpressing Cgb, probably because *E. coli* does not contain an appropriate reductase. The redox potential of Ctb is low when compared to those of other Hbs; the Mbs from the sperm whale, *Aplysia limacina* and Hb from *Chironomus thummi* have potentials of +50, +150, and +120 mV, respectively (*51*). The Hb found in *Lumbricus terrestris* (earthworm) has a midpoint potential of +73 mV (*52*). The bacterial single-domain globin Vgb found in *Vitreoscilla* purifies as a dimer, its two hemes having potentials of +118 and −122 mV (*53*). Further speculation concerning the function of Ctb is, of necessity, limited by the data available.

Conclusions. We report for the first time a detailed characterization of a group III trHb, *C. jejuni* Ctb. Although optical spectra of ferric, ferrous, O_2- and CO-bound forms resemble those of other hemoglobins, resonance Raman analysis shows Ctb to have an atypical ν_{Fe-CO} stretching mode at 514 cm^{-1}, compared to those of the other truncated hemoglobins that have been characterized so far. This implies unique roles in ligand stabilization for TyrB10, HisE7, and TrpG8, residues highly conserved within group III truncated hemoglobins.

ACKNOWLEDGMENT

We thank Guanghui Wu and Karen Elvers for helpful discussions.

SUPPORTING INFORMATION AVAILABLE

Absorbance spectrum of Ctb expressed in vivo in *E. coli*, optical absorption spectra of the ferric protein at pH 7.5 and 10.5, the 1100−1700 cm^{-1} region of the resonance Raman spectrum of the partially photodissociated CO-bound derivative, and the 1500−2140 cm^{-1} region of the resonance Raman spectrum of the partially photodissociated CO-bound derivative. This material is available free of charge via the Internet at http://pubs.acs.org.

REFERENCES

1. Vinogradov, S. N., Hoogewijs, D., Bailly, X., Arredondo-Peter, R., Guertin, M., Gough, J., Dewilde, S., Moens, L., and Vanfleteren, J. R. (2005) Three globin lineages belonging to two structural classes in genomes from the three kingdoms of life, *Proc. Natl. Acad. Sci. U.S.A. 102*, 11385−11389.

2. Wu, G., Wainwright, L. M., and Poole, R. K. (2005) Microbial globins, *Adv. Microb. Physiol. 47*, 255−310.
3. Membrillo-Hernández, J., Coopamah, M. D., Anjum, M. F., Stevanin, T. M., Kelly, A., Hughes, M. N., and Poole, R. K. (1999) The flavohemoglobin of *Escherichia coli* confers resistance to a nitrosating agent, a "nitric oxide releaser," and paraquat and is essential for transcriptional responses to oxidative stress, *J. Biol. Chem. 274*, 748−754.
4. Crawford, M. J., and Goldberg, D. E. (1998) Role for the *Salmonella* flavohemoglobin in protection from nitric oxide, *J. Biol. Chem. 273*, 12543−12547.
5. Liu, L. M., Zeng, M., Hausladen, A., Heitman, J., and Stamler, J. S. (2000) Protection from nitrosative stress by yeast flavohemoglobin, *Proc. Natl. Acad. Sci. U.S.A. 97*, 4672−4676.
6. Poole, R. K., and Hughes, M. N. (2000) New functions for the ancient globin family: bacterial responses to nitric oxide and nitrosative stress, *Mol. Microbiol. 36*, 775−783.
7. Gardner, P. R., Gardner, A. M., Brashear, W. T., Suzuki, T., Hvitved, A. N., Setchell, K. D. R., and Olson, J. S. (2006) Hemoglobins dioxygenate nitric oxide with high fidelity, *J. Inorg. Biochem. 100*, 542−550.
8. Park, K. W., Kim, K. J., Howard, A. J., Stark, B. C., and Webster, D. A. (2002) *Vitreoscilla* hemoglobin binds to subunit I of cytochrome *bo* ubiquinol oxidases, *J. Biol. Chem. 277*, 33334−33337.
9. Elvers, K. T., Wu, G., Gilberthorpe, N. J., Poole, R. K., and Park, S. F. (2004) Role of an inducible single-domain hemoglobin in mediating resistance to nitric oxide and nitrosative stress in *Campylobacter jejuni* and *Campylobacter coli*, *J. Bacteriol. 186*, 5332−5341.
10. Elvers, K. T., Turner, S. M., Wainwright, L. M., Marsden, G., Hinds, J., Cole, J. A., Poole, R. K., Penn, C. W., and Park, S. F. (2005) NssR, a member of the Crp-Fnr superfamily from *Campylobacter jejuni*, regulates a nitrosative stress-responsive regulon that includes both a single-domain and a truncated haemoglobin, *Mol. Microbiol. 57*, 735−750.
11. Pesce, A., Couture, M., Dewilde, S., Guertin, M., Yamauchi, K., Ascenzi, P., Moens, L., and Bolognesi, M. (2000) A novel two-over-two alpha-helical sandwich fold is characteristic of the truncated hemoglobin family, *EMBO J. 19*, 2424−2434.
12. Wittenberg, J. B., Bolognesi, M., Wittenberg, B. A., and Guertin, M. (2002) Truncated hemoglobins: A new family of hemoglobins widely distributed in bacteria, unicellular eukaryotes, and plants, *J. Biol. Chem. 277*, 871−874.
13. Egawa, T., and Yeh, S.-R. (2005) Structural and functional properties of hemoglobins from unicellular organisms as revealed by resonance Raman spectroscopy, *J. Inorg. Biochem. 99*, 72−96.
14. Milani, M., Pesce, A., Ouellet, Y., Ascenzi, P., Guertin, M., and Bolognesi, M. (2001) *Mycobacterium* tuberculosis hemoglobin N displays a protein tunnel suited for O_2 diffusion to the heme, *EMBO J. 20*, 3902−3909.
15. Milani, M., Savard, P. Y., Ouellet, H., Ascenzi, P., Guertin, M., and Bolognesi, M. (2003) A TyrCD1/TrpG8 hydrogen bond network and a TyrB10-TyrCD1 covalent link shape the heme distal site of *Mycobacterium tuberculosis* hemoglobin O, *Proc. Natl. Acad. Sci. U.S.A. 100*, 5766−5771.
16. Hoy, J. A., Kundu, S., Trent, J. T., Ramaswamy, S., and Hargrove, M. S. (2004) The crystal structure of *Synechocystis* hemoglobin with a covalent heme linkage, *J. Biol. Chem. 279*, 16535−16542.
17. Milani, M., Pesce, A., Bolognesi, M., and Ascenzi, P. (2001) Truncated hemoglobins: trimming the classical 'three-over-three' globin fold to a minimal size, *Biochem. Mol. Biol. Edu. 29*, 123−125.
18. Pathania, R., Navani, N. K., Rajomohan, G., and Dikshit, K. L. (2002) *Mycobacterium tuberculosis* hemoglobin HbO associates with membranes and stimulates cellular respiration of recombinant *Escherichia coli*, *J. Biol. Chem. 277*, 15293−15302.
19. Wainwright, L. M., Elvers, K. T., Park, S. F., and Poole, R. K. (2005) A truncated haemoglobin implicated in oxygen metabolism by the microaerophilic food-borne pathogen *Campylobacter jejuni*, *Microbiology (Reading, U.K.) 151*, 4079−4091.
20. Friedman, C. R., Neimann, J., Wegener, H. C., and Tauxe, R. V. (2000) in *Campylobacter* (Nachamkin, I., and Blaser, M. J., Eds.) 2nd ed., pp 121−138, ASM Press, Washington, DC.
21. Pitcher, D. G., Saunders, N. A., and Owen, R. J. (1989) Rapid extraction of bacterial genomic DNA with guanidium thiocyanate, *Lett. Appl. Microbiol. 8*, 151−156.
22. Inoue, H., Nojima, N., and Okayama, H. (1990) High efficiency transformation of *Escherichia coli* with plasmids, *Gene 96*, 23−28.
23. Kalnenieks, U., Galinina, N., Bringer-Meyer, S., and Poole, R. K. (1998) Membrane D-lactate oxidase in *Zymomonas mobilis*: evidence for a branched respiratory chain, *FEMS Microbiol. Lett. 168*, 91−97.
24. Dutton, P. L. (1978) Redox potentiometry: determination of midpoint potentials of oxidation−reduction components of biological electron-transfer systems, *Methods Enzymol. 54*, 411−435.
25. Couture, M., Das, T. K., Lee, H. C., Peisach, J., Rousseau, D. L., Wittenberg, B. A., Wittenberg, J. B., and Guertin, M. (1999) *Chlamydomonas* chloroplast ferrous hemoglobin − Heme pocket structure and reactions with ligands, *J. Biol. Chem. 274*, 6898−6910.
26. Yeh, S. R., Couture, M., Ouellet, Y., Guertin, M., and Rousseau, D. L. (2000) A cooperative oxygen finding hemoglobin from *Mycobacterium tuberculosis* − Stabilization of heme ligands by a distal tyrosine residue, *J. Biol. Chem. 275*, 1679−1684.
27. Lemberg, R., and Barrett, J. (1973) *Cytochromes*, Academic Press, London.
28. Li, X.-Y., and Spiro, T. G. (1988) Is bound CO linear or bent in heme proteins? Evidence from resonance Raman and infrared spectroscopic data, *J. Am. Chem. Soc. 110*, 6024−6033.
29. Ray, G. B., Li, X.-Y., Ibers, J. A., Sessler, J. L., and Spiro, T. G. (1994) How far can proteins bend the FeCO unit? Distal polar and steric effects in heme proteins and models, *J. Am. Chem. Soc. 116*, 162−176.
30. Vogel, K. M., Kozlowski, P. M., Zgierski, M. Z., and Spiro, T. G. (2000) Role of the axial ligand in heme-CO backbonding; DFT analysis of vibrational data, *Inorg. Chim. Acta 297*, 11−17.
31. Mukai, M., Mills, C. E., Poole, R. K., and Yeh, S. R. (2001) Flavohemoglobin, a globin with a peroxidase-like catalytic site, *J. Biol. Chem. 276*, 7272−7277.
32. Antonini, E., and Brunori, M. (1971) *Hemoglobin and Myoglobin in Their Reactions with Ligands*, North-Holland Publishing, Amsterdam, The Netherlands.
33. Poole, R. K., Ioannidis, N., and Orii, Y. (1994) Reactions of the *Escherichia coli* flavohaemoglobin (Hmp) with oxygen and reduced nicotinamide adenine dinucleotide: evidence for oxygen switching of flavin oxidoreduction and a mechanism for oxygen sensing, *Proc. R. Soc. London, Ser. B 255*, 251−258.
34. Couture, M., Yeh, S. R., Wittenberg, B. A., Wittenberg, J. B., Ouellet, Y., Rousseau, D. L., and Guertin, M. (1999) A cooperative oxygen-binding hemoglobin from *Mycobacterium tuberculosis*, *Proc. Natl. Acad. Sci. U.S.A. 96*, 11223−11228.
35. Mukai, M., Savard, P. Y., Ouellet, H., Guertin, M., and Yeh, S. R. (2002) Unique ligand-protein interactions in a new truncated hemoglobin from *Mycobacterium tuberculosis*, *Biochemistry 41*, 3897−3905.
36. Samuni, A., Ouellet, Y., Guertin, M., Friedman, J. M., and Yeh, S.-R. (2004) The absence of proximal strain in the truncated hemoglobins from *Mycobacterium tuberculosis*, *J. Am. Chem. Soc. 126*, 2682−2683.
37. Das, T. K., Weber, R. E., Dewilde, S., Wittenberg, J. B., Wittenberg, B. A., Yamauchi, K., VanHauwaert, M. L., Moens, L., and Rousseau, D. L. (2000) Ligand binding in the ferric and ferrous states of *Paramecium* hemoglobin, *Biochemistry 39*, 14330−14340.
38. Friedman, J. M., Scott, T. W., Stepnoski, R. A., Ikeda-Saito, M., and Yonetani, T. (1983) The iron-proximal histidine linkage and protein control of oxygen binding in hemoglobin. A transient Raman study, *J. Biol. Chem. 258*, 10564−10572.
39. Couture, M., Das, T. K., Savard, P. Y., Ouellet, Y., Wittenberg, J. B., Wittenberg, B. A., Rousseau, D. L., and Guertin, M. (2000) Structural investigations of the hemoglobin of the cyanobacterium *Synechocystis* PCC6803 reveal a unique distal heme pocket, *Eur. J. Biochem. 267*, 4770−4780.
40. Ouellett, H., Ouellett, Y., Richard, C., Labarre, M., Wittenberg, B., Wittenberg, J., and Guertin, M. (2002) Truncated hemoglobin HbN protects *Mycobacterium bovis* from nitric oxide, *Proc. Natl. Acad. Sci. U.S.A. 99*, 5902−5907.
41. Mukai, M., Ouellet, Y., Ouellet, H., Guertin, M., and Yeh, S. R. (2004) No binding induced conformational changes in a truncated hemoglobin from *Mycobacterium tuberculosis*, *Biochemistry 43*, 2764−2770.
42. Crespo, A., Marti, M. A., Kalko, S. G., Morreale, A., Orozco, M., Gelpi, J. L., Luque, F. J., and Estrin, D. A. (2005) Theoretical study of the truncated hemoglobin HbN: Exploring the molecular

basis of the NO detoxification mechanism, *J. Am. Chem. Soc. 127*, 4433−4444.
43. Ouellet, H., Juszczak, L., Dantsker, D., Samuni, U., Ouellet, Y. H., Savard, P. Y., Wittenberg, J. B., Wittenberg, B. A., Friedman, J. M., and Guertin, M. (2003) Reactions of *Mycobacterium tuberculosis* truncated hemoglobin O with ligands reveal a novel ligand-inclusive hydrogen bond network, *Biochemistry 42*, 5764−5774.
44. Giangiacomo, L., Ilari, A., Boffi, A., Morea, V., and Chiancone, E. (2005) The truncated oxygen-avid hemoglobin from *Bacillus subtilis* − X-ray structure and ligand binding properties, *J. Biol. Chem. 280*, 9192−9202.
45. Liu, C., He, Y., and Chang, Z. Y. (2004) Truncated hemoglobin *o* of *Mycobacterium tuberculosis*: the oligomeric state change and the interaction with membrane components, *Biochem. Biophys. Res. Commun. 316*, 1163−1172.
46. Ascenzi, P., Bocedi, A., Bolognesi, M., Fabozzi, G., Milani, M., and Visca, P. (2006) Nitric oxide scavenging by *Mycobacterium leprae* GlbO involves the formation of the ferric heme-bound peroxynitrite intermediate, *Biochem. Biophys. Res. Commun. 339*, 450−456.
47. D'mello, R., Hill, S., and Poole, R. K. (1995) The oxygen affinity of cytochrome *bo*′ in *Escherichia coli* determined by the deoxygenation of oxyleghemoglobin and oxymyoglobin: K_m values for oxygen are in the submicromolar range. *J. Bacteriol. 177*, 867−870.
48. D'mello, R., Hill, S., and Poole, R. K. (1996) The cytochrome *bd* quinol oxidase in *Escherichia coli* has an extremely high oxygen affinity and two oxygen-binding haems: implications for regulation of activity in vivo by oxygen inhibition, *Microbiology 142*, 755−763.
49. Pesci, E. C., Cottle, D. L. and Pickett, C. L. (1994) Genetic, enzymatic and pathogenic studies of the iron superoxide dismutase of *Campylobacter jejuni*, *Infect. Immun. 62*, 2687−2694.
50. Frey, A. D., Farres, J., Bollinger, C. J. T., and Kallio, P. T. (2002) Bacterial hemoglobins and flavohemoglobins for alleviation of nitrosative stress in *Escherichia coli*, *Appl. Environ. Microbiol. 68*, 4835−4840.
51. Brunori, M., Saggese, U., Rotilio, G. C., Antonini, E., and Wyman, J. (1971) Redox equilibrium of sperm-whale myoglobin, *Aplysia* myoglobin and *Chironomus thummi* hemoglobin, *Biochemistry 10*, 1604−1609.
52. Dorman, S. C., Harrington, J. P., Martin, M. S., and Johnson, T. V. (2004) Determination of the formal reduction potential of *Lumbricus terrestris* hemoglobin using thin layer spectroelectrochemistry, *J. Inorg. Biochem. 98*, 185−188.
53. Tyree, B., and Webster, D. A. (1978) Electron-accepting properties of cytochrome *o* purified from *Vitreoscilla*, *J. Biol. Chem. 253*, 7635−7637.

BI052247K